Dynamics of excitons in CuBr nanocrystals: Spectral-hole burning and transient four-wave-mixing measurements

J. Valenta,* J. Moniatte, P. Gilliot, B. Hönerlage, J. B. Grun, and R. Levy
Institut de Physique et Chimie des Matériaux de Strasbourg (UM 380046, CNRS-ULP-EHICS), Groupe d'Optique Nonlinéaire et d'Optoélectronique, 23 rue du Loess, 67037 Strasbourg Cedex 02, France

A. I. Ekimov
A. F. Ioffe Physico-Technical Institute, 194021 St. Petersburg, Russia
(Received 26 March 1997; revised manuscript received 30 June 1997)

CuBr nanocrystals (NC's) embedded in a borosilicate glass matrix have been studied by transmission pump-and-probe experiments with both spectral and temporal resolution. Transient as well as persistent spectral hole-burning phenomena are observed in the excitonic absorption of small NC's (mean radius less than 4 nm) when picosecond and nanosecond dye-laser pulses excite selectively NC's of a specific size at low temperatures. The holes consist of a zero-phonon line (at the photon energy of the excitation) and marked phonon sidebands. This structure is explained by a strong exciton–optical-phonon interaction. A value of about 1 of the Huang-Rhys factor S is obtained from the Stokes shifts between absorption and photoluminescence spectra. From the width of zero-phonon holes, a lower limit of 2.3 ps of the exciton dephasing time T_2 is deduced. This value is compared to the one obtained by transient four-wave-mixing measurement (6.4 ps) at low excitation intensities. When the radii of NC's decrease, both types of spectral holes become broader and the persistent spectral-hole burning is more efficient. [S0163-1829(98)07903-X]

I. INTRODUCTION

Transient spectral-hole burning (SHB) was initially observed in low-dimensional semiconductors (nanocrystals) at the end of the 1980s. This phenomenon generally has been explained by the selective saturation of the electronic transitions of a part of the semiconductor nanocrystallites (NC's), within the spectrally inhomogeneous broadband that results from their size distribution. Decay times ranging from picoseconds[1] to hundreds of nanoseconds were reported.[2,3]

On the other hand, persistent SHB was initially observed only in four types of inorganic materials (color centers, divalent rare-earth ions in crystals, transition-metal ions in crystals, and rare-earth ions in glasses[4]) when Masumoto and co-workers reported two years ago similar effects in the lowest excitonic absorption band of CdSe, $CdSe_xSe_{1-x}$, CuCl, CuBr, and CuI nanocrystals dispersed in glasses or crystalline matrices.[5] They concluded that, in spite of the relatively large number of atoms (greater than 10^3) in the nanocrystals, the surface plays an important role and the ground state of crystallite-matrix complexes therefore can be highly degenerate. Although many studies have been performed on NC's and plausible models proposed, still many questions remain open concerning crystallite-matrix interactions, exciton-phonon interactions, homogeneous linewidths, etc.

Here we will first explain what we mean by the terms ''persistent'' and ''transient'' SHB. Persistent changes of absorption last (after the end of excitation) for a time significantly longer than the lifetime of any elementary excitations (typically tens of minutes or hours at very low temperatures), while transient effects involve changes that exist only during the lifetime of the excited states, i.e., hundreds of nanoseconds or even shorter.

The scope of this work is first to compare transient and persistent SHB phenomena observed by pump-and-probe experiments in CuBr NC's (Secs. IV A–IV C) and second to deduce the characteristic dephasing time T_2 of excited states (Sec. IV D). The values obtained by SHB are compared to those obtained by direct time-resolved transient four-wave-mixing (TFWM) measurements. In Sec. IV E we analyze the spectral shape of SHB spectra in order to study exciton-phonon interactions in these NC's. Also the temperature dependence of spectral holes (SH's) has been observed (Sec. IV F). Mechanisms of both transient and persistent SHB are discussed in Sec. V.

II. EXPERIMENTAL CONDITIONS

Light-induced absorption changes, Raman scattering, and degenerate four-wave-mixing experiments were all performed at low temperatures, the samples being cooled down inside a continuous-flow cryostat or in a helium-bath cryostat with windows made of fused silicate glass. For experiments in the picosecond time range, we used as pump light source a dye-laser with PBBO in dioxane as the active medium, synchronously pumped by the third harmonics of an active/passive mode-locked Nd:YAG laser (where YAG denotes yttrium aluminum garnet) tuned by a grating in a Littrow mount. Pulses about 20 ps in duration and 0.3 meV spectral width [full width at half maximum (FWHM)] were generated with a 5-Hz repetition rate. For nanosecond experiments, the pump source was a dye laser with a grating at grazing incidence in its cavity, pumped transversally by the XeCl excimer laser radiation.[6] The spectral width of the laser emission was less than 0.05 meV (FWHM) and the pulse duration was between 5 and 10 ns. The same dye laser was used to measure the resonant Raman scattering in CuBr NC's.

Absorption changes were tested with the spectrally broad superradiance of a dye excited by a part of the laser source emission, i.e., the Nd:YAG laser and the XeCl excimer laser for picosecond and nanosecond experiments, respectively. The corresponding superradiant emissions had a time duration of about 20 ps and 2 ns, respectively. The test pulses were sent through an optical delay line that permits one to adjust the delay between the pump and the probe pulses in the transient SHB experiments. The test pulses that spectrally cover the excitonic absorption of the NC's were dispersed in a single grating $\frac{3}{4}$-m Spex monochromator (working either in the first or the second order of diffraction) and detected by an optical multichannel analyzer connected to a computer. The nanosecond system has a better stability than the picosecond one; it permits one to detect absorption changes $\Delta\alpha/\alpha$ of about 1%.

The photoluminescence (PL) emitted by the samples was excited by means of the XeCl excimer laser ($\lambda = 308$ nm, 20-ns pulse duration) and detected in 45° geometry. The linear absorption of the samples at low temperatures was measured using a tungsten lamp. For both PL, a photomultiplier tube connected to a boxcar integrator was used for the detection of the light dispersed by the monochromator.

We used a self-mode-locked Ti:sapphire laser to perform TFWM experiments in the usual two-beam configuration. Light pulses of 400 nm wavelength with a 2.5 nm width were obtained by frequency doubling 80-fs pulses of 800 nm wavelength. The outgoing beam was further split into two parts that impinged on the samples with $\mathbf{k}_1$ and $\mathbf{k}_2$ wave vectors. The signal was detected with a photomultiplier and a lock-in amplifier in the $2\mathbf{k}_2$-$\mathbf{k}_1$ direction as a function of the delay τ between the pulses of the two beams. We checked that no effects were due to the high repetition rate (82 MHz) of the laser by reducing it to 4 MHz with a pulse picker.

III. SAMPLES

The CuBr nanocrystals were grown in a borosilicate glass matrix using a diffusion controlled process.[7] The semiconductor concentration in the matrix is about 1% and the thickness of the samples is typically about 0.4 mm. We studied five samples made of glass containing CuBr NC's of different mean radii: 12, 9.5, 5.1, 3.9, and 2.8 nm (the exciton Bohr radius in bulk CuBr is 1.25 nm). The crystal structure of CuBr NC's is cubic (zinc blende). The linear absorption spectra of all these samples at room temperature are shown in Fig. 1.

The existence of the excitonic absorption ($Z_{1,2}$ and Z_3 bands) at room temperature as well as the strong blueshift with decreasing radius of NC's can be noted. The mean radius of the NC's was determined from the spectral positions of the maxima of the $Z_{1,2}$ and Z_3 excitonic absorption bands using the donorlike exciton model.[8]

IV. RESULTS

A. Linear absorption, photoluminescence, and Raman scattering

The linear absorption and photoluminescence spectra, at 2 K, of a sample containing 2.8-nm CuBr NC's are shown in Fig. 2, curves A and B, respectively. The poor efficiency of the luminescence in our excitation conditions should be noticed ($\lambda_{exc}=308$ nm, $h\nu_{exc}=4.024$ eV, and the lowest excitation intensity necessary to obtain a signal-to-noise ratio high enough to permit a measurement is 20 kW cm^{-2}). Because of the vicinity of the absorption and the emission bands, a strong reabsorption affects the emission spectrum. Therefore, we calculate the spectral shape of the reabsorption-free emission $I_L^0(h\nu)$. Neglecting reflection losses, we assume an exponential decrease inside the sample of the exciting radiation and the resulting emission (the effect of the subsequent reabsorptions of the reemitted light can be neglected as the efficiency of emission is low):

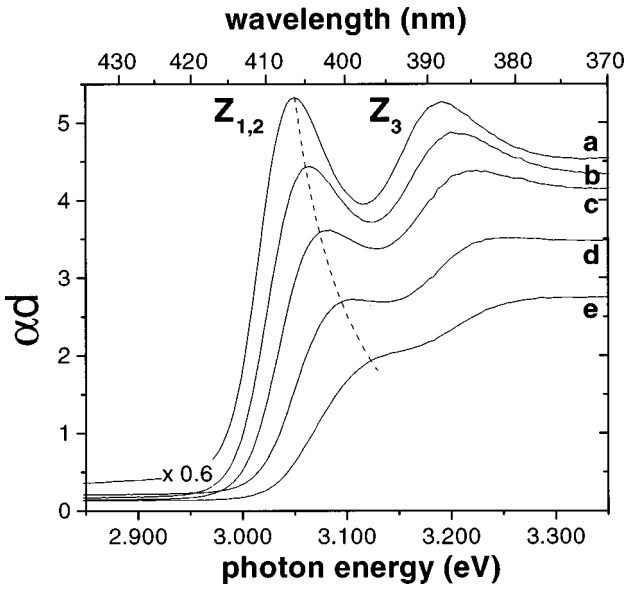

FIG. 1. Linear absorption spectra (at room temperature) of glass samples containing CuBr NC's of the following mean radii: (a) 12, (b) 9.5, (c) 5.1, (d) 3.9, and (e) 2.8 nm. The absorption bands labeled $Z_{1,2}$ and Z_3 correspond to the lowest excitonic states of CuBr.

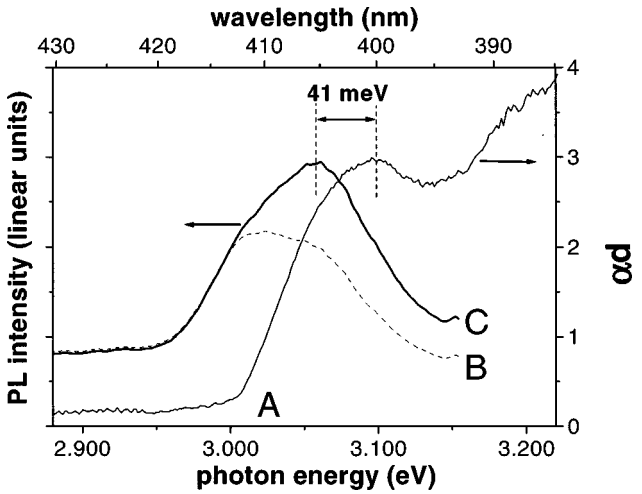

FIG. 2. Linear absorption spectrum (A), photoluminescence (PL) spectrum (B), and PL spectrum once corrected for reabsorption (C) using Eq. (1) for a sample of glass doped with CuBr NC's of 2.8 nm mean radius (2 K). The PL is excited by an excimer laser (laser photon energy 4.024 eV and intensity 50 kW cm^{-2}).

$$I_L^0(h\nu) \propto \frac{I_L^m(h\nu)[\alpha(h\nu)+\alpha(h\nu_{\rm exc})]}{1-\exp\{-[\alpha(h\nu)+\alpha(h\nu_{\rm exc})]d\}}, \quad (1)$$

where $I_L^m(h\nu)$ is the emission intensity of the sample excited at $h\nu_{\rm exc}$ measured at the $h\nu$ photon energy. $\alpha(h\nu)$ and $\alpha(h\nu_{\rm exc})$ are the absorption coefficients of the sample at $h\nu$ and $h\nu_{\rm exc}$ and d is its thickness. The PL spectrum once corrected (Fig. 2, curve *C*) has its maximum at about 3.059. It can be related to the radiative recombination of excitons (*X* line).

The Stokes shift Δ_S between the maxima of the excitonic absorption and emission is 41 ± 6 meV. Under the condition that the position of the *X* band is not redshifted by localization of excitons in impurity or surface states [important in small NC's (Ref. 9)], the Stokes shift Δ_S may be related to the Huang-Rhys factor *S* (which characterizes the importance of the exciton-phonon interaction) and to the energy of the coupled LO-phonon $\hbar\Omega$:[10]

$$\Delta_S = 2S\hbar\Omega. \quad (2)$$

If we take as the energy of the LO phonon the value 20.15 ± 0.3 meV we obtained by resonant Raman scattering (see below) in the 2.8-nm NC's of CuBr, we find a Huang-Rhys factor $S=1.02\pm0.15$. It is quite high, indicating that the exciton–LO-phonon interaction is important in this polar material, as already seen in the single- and two-photon absorption spectra of the exciton in bulk CuBr.[11,12]

Resonant Raman scattering due to exciton-phonon interactions was measured using the nanosecond dye laser. The one LO and two LO-phonon lines were observed only when the laser photon energy was tuned in the exciton resonance, as can be seen in the excitation spectrum of the LO-phonon Raman line [Fig. 3(a)]. Its maximum is only slightly redshifted compared to the excitonic absorption. Through the entire range of resonant Raman scattering, the Stokes shift of the LO line remains constant within our experimental precision [Fig. 3(b)]. The value of $\hbar\Omega_{\rm LO}=20.15\pm0.3$ meV is slightly smaller than the $\hbar\Omega_{\rm LO}=20.7$ meV in bulk CuBr.

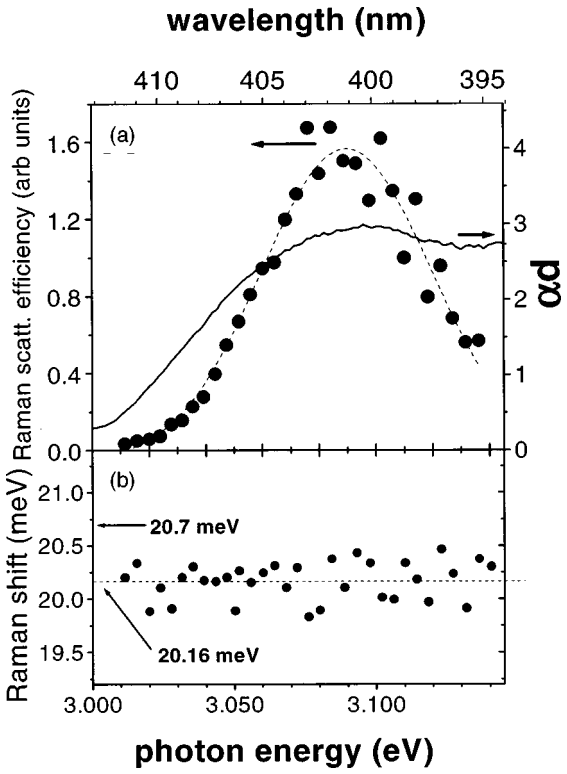

FIG. 3. Resonant Raman scattering of the same sample of glass doped with 2.8-nm CuBr NC's in the same conditions of excitation as discussed in Fig. 2. (a) Excitation spectrum of the LO-phonon Raman line (full circles); the linear absorption spectrum is plotted (continuous line) for comparison. (b) Stokes shift of the LO-phonon Raman line for different photon energies of the exciting laser.

B. Transient changes of absorption

1. Nanocrystals of large sizes

First we present the results of pump-and-probe experiments performed with the picosecond setup on big nanocrystals, i.e., NC's with mean radii 12, 9.5, and 5.1 nm. All these samples display similar excitonic absorption changes under resonant excitations in the $Z_{1,2}$ excitonic band. These effects are shown in Fig. 4 for 9.5-nm NC's. They are measured at different peak intensities (10, 20, and 40 MW cm^{-2}) for a 3.026-eV picosecond pulsed excitation, at 2 K.

The main features of the observed absorption changes can be summarized as follows. (i) The absorption changes are almost independent of the photon energy of the exciting laser. They always start on the low-energy side of the absorption band and reach the same shape for the highest intensity of excitation [Fig. 4(a)]. (ii) Both the $Z_{1,2}$ and the Z_3 absorption bands blueshift and broaden and their spectrally integrated intensities diminish when the intensity of the resonant excitation increases. This gives a typical shape for the differential absorption spectra [Fig. 4(b)]. (iii) In contrast to the Z_3 band, a structure is clearly observed in the differential absorption of the $Z_{1,2}$ band. Two subbands peak up at 3.00 and 3.02 eV. They are separated by about 20 meV.

Such effects have been observed by Woggon, Henneberger, and Müller[13] and are very similar to the behavior of CuCl NC's in a glass matrix.[14] They have been qualitatively well explained in the framework of a time-dependent Hartree-Fock theory as being due to exciton-exciton interactions[14–16] that increase the exciton energy and therefore cause a blueshift of the excitonic absorption band.

The dynamics of the absorption changes in the $Z_{1,2}$ exciton band is shown in Fig. 5 for the same sample at 2 K. The excitation is provided by a picosecond laser pulse of 3.02-eV photon energy and 4-MW cm^{-2} intensity. In Fig. 5 (top) we have drawn the differential absorption spectra measured at different delays after the temporal coincidence of the pump and the probe pulses. One can see that the maximum of the bleaching shifts towards lower energies versus time, the exciton line returning then from a blueshifted position. In Fig. 5 (bottom) we have plotted the temporal evolution of the differential absorption at two different photon energies (2.982 and 2.996 eV), chosen in the two low-energy subbands and far from the excitation photon energy. For both photon energies, in addition to a fast response that follows the exciting laser pulse, a very slow decay with a characteristic time in the range 1–100 ns can be seen. The fast signal, which is more intense at 2.996 eV than at 2.982 eV, may be related to the blueshift of the exciton band. It may correspond to the creation of two (or more) excitons per crystallite

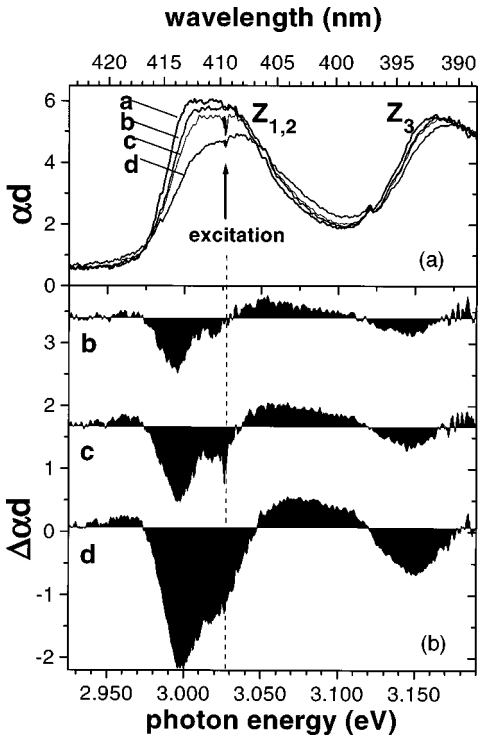

FIG. 4. Spectra of transient absorption changes for a sample of glass doped with large CuBr NC's (9.5 nm) at 2 K under a resonant picosecond excitation (3.026 eV) of intensity (*a*) 0 (linear absorption), (*b*) 10, (*c*) 20, and (*d*) 40 MW cm^{-2}. (a) Absorption spectra and (b) corresponding differential absorption spectra (black areas of the graphs).

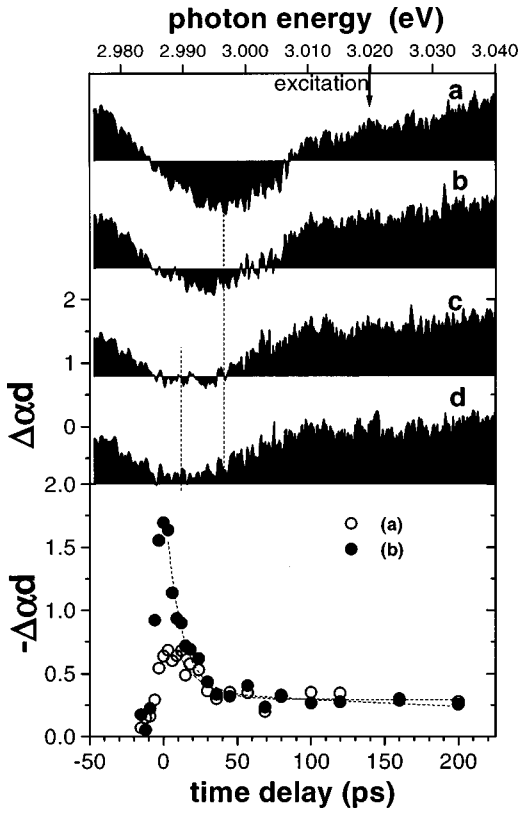

FIG. 5. Dynamics of the absorption changes in the same experimental conditions and for the same sample as in Fig. 4: In the upper part, four differential absorption spectra (black areas of the graphs) represent the absorption changes probed after the following delays τ: (*a*) 0, (*b*) 6, (*c*) 12, and (*d*) 16 ps after the maximum of the pump pulse intensity. In the lower part, temporal changes of absorption at two photon energies (○) 2.982 eV (at the edge of the absorption band) and (●) 2.996 eV (at the maximum of the absorption changes) are shown.

and to their fast recombination through very rapid exciton-exciton scattering processes since exciton-exciton interactions are at the origin of the exciton blueshift, as is theoretically shown. The slow absorption changes may then correspond to the decay of single excitons created per crystallite.

In these samples containing large size nanocrystals, the pump-and-probe experiments performed with nanosecond dye lasers give essentially the same results as with picosecond ones.

2. Nanocrystals of small sizes

The nonlinear absorption first measured with the picosecond setup is different for NC's with mean radii smaller than about 4 nm. In addition to spectrally broad absorption changes due to the shift of the absorption band and very similar to those observed in large NC's, a narrow hole is burnt at the spectral position of the pump even at low excitation intensity [Figs. 6(a) and 6(b)]. When we increase the excitation intensity, the spectral hole widens and spectrally broad absorption changes appear and increase, so that finally, at 40 MW cm^{-2}, the absorption band becomes almost completely bleached. When we change the laser wavelength, the narrow spectral hole follows the laser position.

The dynamics of the corresponding differential absorption, measured at two different photon energies (3.034 and 3.003 eV), is given in Fig. 7. At 3.003 eV, close to the excitation photon energy 3.001 eV, in addition to a fast response that follows the exciting laser pulse, an exponential decay with a 130 ± 20 ps time constant is obtained. At 3.034 eV, only the slower response is observed. The fast dynamics could be related, as for large NC's, to the creation of two or more excitons per crystallite. The longer decay time of about 130 ps could correspond, as for larger NC's, to the lifetime of a population of excitons when there is only one per crystallite. Their lifetime, however, would be shorter than expected for crystallites of smaller sizes. Quasiparticles from this population of weakly interacting excitons that have such a size that their energies correspond to the exciting photon energy may be involved in the SHB effect.

From the results presented in Fig. 6, it clearly appears that to study pure spectral-hole-burning effects in small NC's one has to use low-excitation intensities. For this purpose, the nanosecond dye laser was more suitable because it has a better pulse intensity stability and a narrower spectral width than the picosecond ones.

We should mention that, in addition to transient effects, persistent absorption changes are also observed. As they are generally proportional to the integrated energy deposited in the sample, these persistent changes are more intense in the case of excitation by more energetic nanosecond laser pulses. We will describe these phenomena in the following subsections.

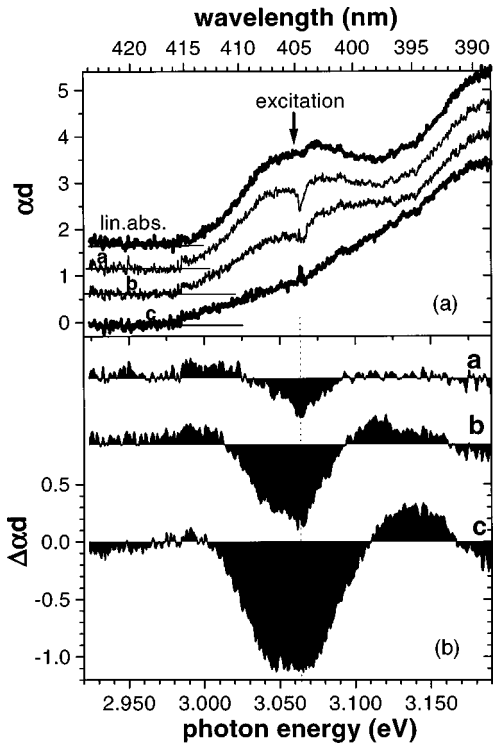

FIG. 6. Spectra of transient absorption changes of a sample with small CuBr NC's (2.8 nm and 2 K) under a picosecond resonant (at 3.064 eV) excitation of intensities (*a*) 2.5, (*b*) 10, and (*c*) 40 MW cm^{-2}. The upper part (a) represents the absorption spectra, while the lower part (b) shows the corresponding differential absorption spectra (black areas of the graphs). Small persistent absorption changes remain once the excitation (40 MW cm^{-2}) has ended, as can be seen in (a).

C. Persistent spectral-hole burning

1. Separation of transient and persistent effects

The transient and the persistent changes of absorption are produced simultaneously during the pump laser excitation (and they are of the same order of magnitude at the early stage of the excitation). The separation of the two effects can therefore be made only approximately.

With the nanosecond setup, we probe the transmission of the samples with nanosecond test pulses at the following times: before any excitation (i.e., virgin sample), during a nanosecond excitation, and after the end of the excitation (i.e., after a delay of several seconds, the time necessary for data acquisition to be completed, which is typically about 25 s). The persistent SHB spectra can be easily deduced from the comparison of the sample transmission measured before and after the excitation. On the other hand, the transient SHB, when determined from the transmission measured during and after the excitation (i.e., including persistent changes), is not correctly determined at the early stage of the excitation of persistent effects, when only a small fluence (i.e., integrated energy by unit area) of light has been sent onto the sample, since then persistent effects are developing rapidly. One can notice, however, that, after having sent onto the sample a fluence of about 0.1 mJ cm^{-2}, persistent changes grow slowly. Therefore, the described procedure to separate the transient from the persistent changes becomes then reasonably correct. In Fig. 8 (absorption spectra) and Fig. 9 (differential absorption spectra), we show (a) five transient and (b) five persistent spectra measured for different pulse energies (excitation densities) and different fluences, respectively, at 2 K. They have been separated following the

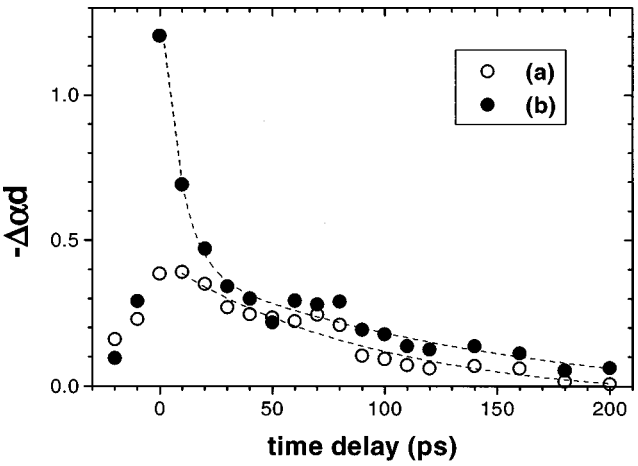

FIG. 7. Dynamics of absorption changes in the sample with small CuBr NC's (2.8 nm) under picosecond excitation at 3.001 eV, at two photon energies 3.034 eV (○) (far from the excitation) and 3.003 eV (●) (near the exciting laser energy). The dashed curves correspond to a double exponential decay with the characteristic times 20 and 130±20 ps.

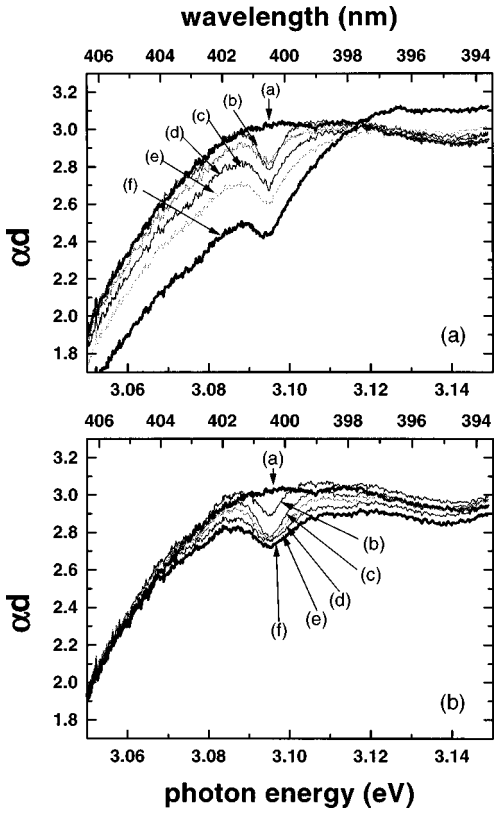

FIG. 8. $Z_{1,2}$ excitonic absorption bands of CuBr nanocrystals of 2.8 nm mean radius, at 2 K, under a resonant excitation by a nanosecond dye laser, in the (a) transient and (b) persistent regimes. The linear spectrum is denoted (*a*). The different exciting pulse energies are (*b*) 23, (*c*) 57, (*d*) 140, (*e*) 230, and (*f*) 570 nJ and the different fluences are (*b*) 6.1, (*c*) 55, (*d*) 150, (*e*) 650, and (*f*) 1030 μJ cm^{-2}.

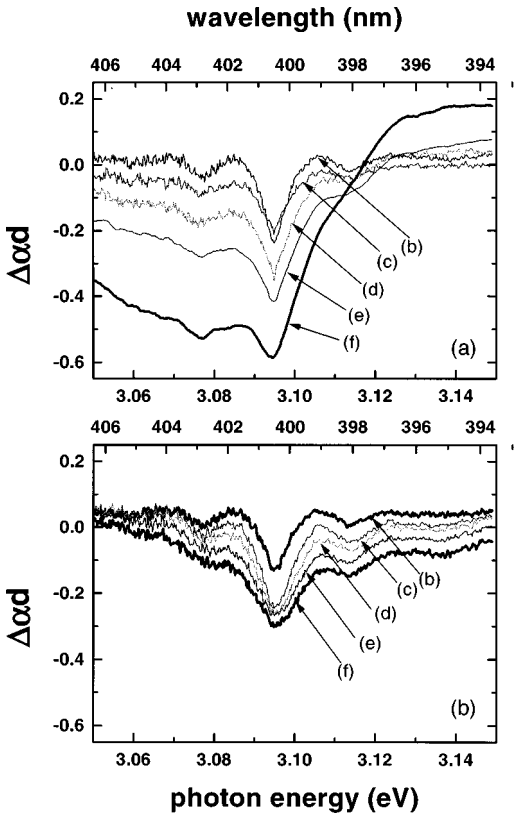

FIG. 9. Differential absorption spectra of the preceding $Z_{1,2}$ excitonic absorption band of the 2.8-nm CuBr NC's, given in Fig. 8, in the (a) transient and (b) persistent regimes (2 K).

method described above. The spectral shapes of both the transient and the persistent SHB's are mainly the same (to be discussed in Sec. IV D), the differences being essentially in the background changes.

Large persistent SHB spectra (Fig. 10) reveal that the narrow spectral holes are accompanied by an induced absorption peaked at 3.03 and 3.30 eV (below excitonic resonances). In Fig. 10, graphs (a) and (b) correspond to the absorption changes induced by an excitation in the $Z_{1,2}$ and Z_3 excitonic bands, respectively. The differential absorption is similar in both cases, but the fine structure clearly observed near the excitation wavelength when the sample is excited in the $Z_{1,2}$ excitonic resonance (a) is smoothed out when the Z_3 resonance is excited (b). A separation observed between induced bleaching and darkening is relatively large, indicating that the mechanism of persistent SHB is probably photochemical.[10]

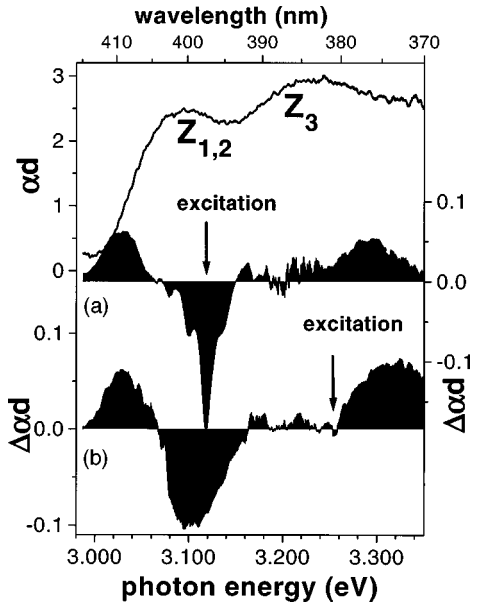

FIG. 10. Differential absorption spectra of the preceding sample (with small 2.8-nm CuBr NC's) for two exciting photon energies: (a) 3.12 eV and (b) 3.25 eV. The linear absorption spectrum is plotted as a continuous line for comparison (2 K).

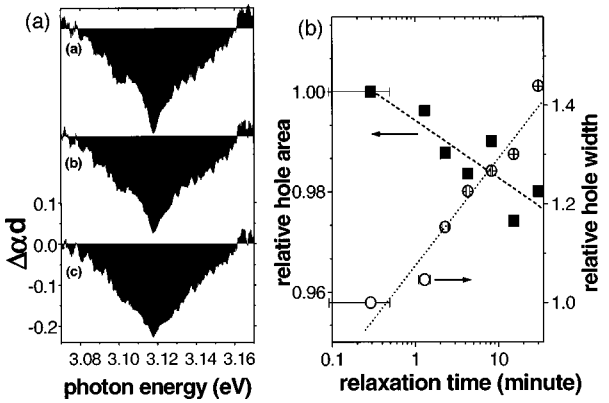

FIG. 11. Spontaneous filling of persistent SHB's in small 2.8-nm CuBr NC's. (a) Holes measured at three different delays after their burning (from top to bottom): (a) 5–35 s, (b) 4–4.5 min, and (c) 30–30.5 min. (b) Semilogarithmic plot of the hole area (full squares) and width (open circles) vs relaxation time.

2. Growth and decay of persistent spectral holes

The central depths of persistent SH's grow approximately as the logarithm of the fluence, but their width increase only slightly even when the fluence is increased from mJ cm^{-2} to J cm^{-2}. In order to evaluate the persistency of spectral holes, we measured their relaxation time after being burnt. It is the so-called spontaneous hole filling (HF), i.e., the disappearance of the spectral hole without any applied external perturbation such as thermal heating (thermally induced HF) or exposure to light (light-induced HF). We observe a slow logarithmic type of temporal recovery of the hole parameters (Fig. 11). The decrease of the spectrally integrated central part of the holes is about 4% in 30 min. The spectral broadening of the holes is also non-negligible and increases logarithmically with time. The detailed study of hole-filling effects (including thermally and laser-induced HF) of persistent SH's in CuBr NC's is published separately.[17]

D. Dephasing time determined from central hole width and TFWM measurements

In transient SHB, the spectrally narrow central hole has generally a Lorentzian spectral shape for low excitations. When we fit the holes (FWHM) by such a shape at different pump intensities, the δ_0 limit value of the linewidth at zero fluence or zero intensity is twice the FWHM homogeneous γ_h linewidth and can be related to the transverse T_2 relaxation time (total dephasing time) through the expression[18]

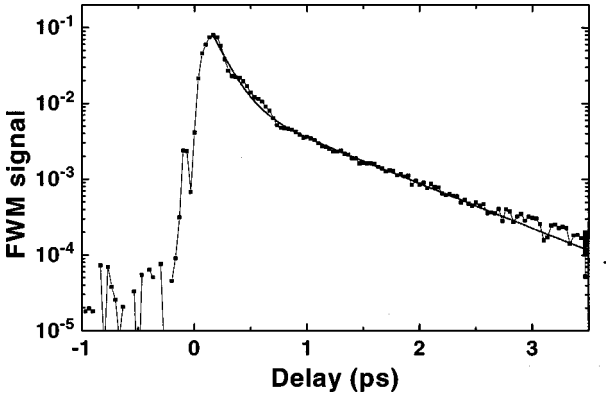

FIG. 12. TFWM signal plotted as a function of the delay τ between the pulses of the two incident pump beams for small 2.8-nm CuBr NC's at 5 K. The central photon energy of the incident pulses is resonant with the Z_{12} excitonic line (3.099 eV) and the fluence is 0.4 μJ/cm^{-2}. The dotted curve represents the experimental data and the full line curve its fit by a double exponential function with two decay parameters 0.74 and 0.13 ps.

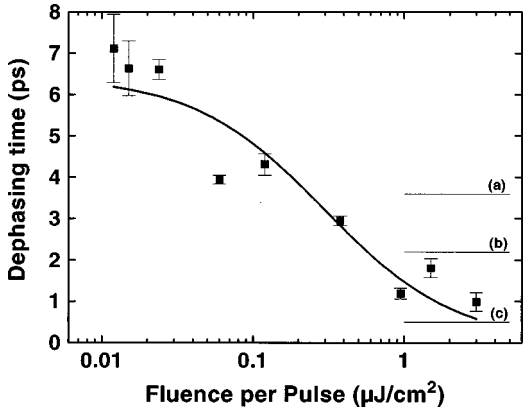

FIG. 13. Dephasing time T_2 determined from the TFWM experiment plotted as a function of the excitation fluence. The continuous curve represents a fit used to determine the low-fluence limit T_2^0 (see the text). Lines $(a)-(c)$ show the values determined from the SHB experiments at the photon energies (a) 3.091 eV, (b) 3.061 eV, and (c) 3.139 eV.

$$\delta_0 = 2\gamma_h = 4\hbar / T_2 . \tag{3}$$

We perform SHB measurements at different spectral positions of the pump-laser excitation inside the inhomogeneously broadened $Z_{1,2}$ exciton absorption band of samples containing NC's of 2.8 nm mean radius (i.e., we excite selectively NC's of different sizes). At each spectral position of the excitation a transient and a persistent hole are burnt at each pulse intensity and fluence. Each hole can be fitted by a Lorentzian line shape. In order to eliminate the intensity broadening, we extrapolate the hole width to zero intensity and zero fluence. The spectral width of the laser being less than 0.05 meV, the spectral resolution of the setup is given by spectrometer and is 0.2 meV. This value has to be subtracted from the hole width we measure experimentally to obtain the real burnt hole width.

We obtained a hole width δ_0 of 0.74 meV for an exciton photon energy $h\nu = 3.091$ eV. Using Eq. (3), it gives $T_2 \geqslant 3.6$ ps as the lower limit of the exciton transverse relaxation time. For $h\nu = 3.061$ eV, $\delta_0 = 1.24$ meV and $T_2 \geqslant 2.2$ ps; for $h\nu = 3.139$ eV, $\delta_0 = 5.21$ meV, and $T_2 \geqslant 0.5$ ps.

One can see that the hole width strongly increases and therefore the corresponding dephasing time calculated [Eq. (3)] strongly decreases when the samples are excited on the high photon energy side of the Z_{12} excitonic band ($h\nu = 3.139$ eV), i.e., for decreasing radii of NC's. This effect corresponds to an increase of the damping of the exciton states, which can be explained by a fast energy relaxation of quasiparticles when on the higher-energy states. In this case, more relaxation channels are available than in the exciton ground state.

These dephasing times can be compared with those measured on the same sample by a TFWM experiment. Figure 12 shows the signal intensity plotted as a function of the delay between the pulses of the two incident beams. This curve corresponds to a double exponential decay. The origin of the very first fast time decay remains unclear. As the excitonic band, in which the sample is resonantly excited, is inhomogeneously broadened, the TFWM signal can be seen as a photon echo. We then determine the coherence time T_2 by multiplying the slow decay time component by a factor 4.

We find by extrapolation T_2^0 at zero intensity and zero fluence (Fig. 15) by using the simple intensity-dependent expression

$$\frac{1}{T_2(I)} = \frac{1}{T_2^0} + \beta I. \tag{4}$$

The value $T_2^0 = 6.4$ ps of the coherence time we determine by TFWM is larger than the one obtained by the SHB technique (Fig. 13). This discrepancy can be explained by comparing fluences and intensities of the incident beams in each experiment: a maximum of 3 μJ cm^{-2} for the TFWM and about 100 μJ cm^{-2} for the SHB. The nonlinear mechanisms involved in SHB suppose, as a matter of fact, higher excitonic populations in order to induce saturations and absorption changes. These populations give rise to a broadening of the line that remains even if we consider the extrapolation of hole width to the zero fluence. In SHB experiments the transitions need to be saturated and the value of $2\gamma_h$ [Eq. (3)] for the hole width is given by a low-intensity extrapolation. In that low-intensity limit the broadening due to exciton collisions is still contributing. On the other hand, γ_h can be directly measured in four-wave-mixing experiments. The low-fluence limit in that case corresponds to the extinction of the excitonic collisions. Another reason for the discrepancy can be the broadening of the central hole by unresolved phonon sidebands, involving low-frequency phonons such as confined acoustic phonons.

The TFWM experiment performed with femtosecond pulses had no spectral resolution. Therefore, we measure a mean T_2 time, averaged over NC's of different sizes. The very-low-excitation intensity used in TFWM experiments, however, permits one to perform more precise measurements of the coherence time and the homogeneous linewidth than saturation spectroscopy such as SHB, which needs high fluences.

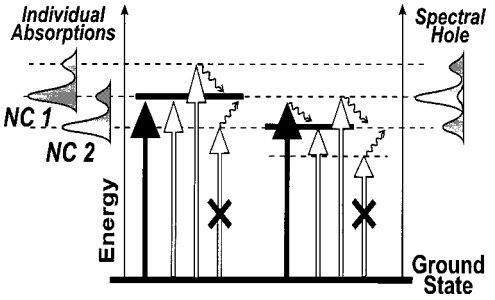

FIG. 14. Schema of the different transitions involved to explain the SHB structures, i.e., the central holes and their sidebands. The black arrows represent the intense pump excitation of the NC's, the gray ones the probing of these NC's absorption by the test pulses. Absorption processes including one-phonon absorption are forbidden at low temperature.

E. Spectral shape of hole-burning structures

Both transient and persistent SH's (see Fig. 9) are composed of a central hole at the spectral position of the exciting laser and from several sidebands on its high-energy as well as low-energy side. Now we would like to discuss the origin of the two deepest sidebands observed in the hole spectra. The energy separation $\Delta \sim 19$ meV between the high-energy sideband and the main hole is only slightly less than the LO-phonon energy we measured by resonant Raman scattering (20.15 meV). Therefore, we attribute this sideband to a LO-phonon replica in absorption spectrum of NC's of specific size (see Fig. 14). This means that when NC's of a distinct size are selectively excited by the pump beam, all the absorptions related to these NC's are removed from the inhomogeneously broadened exciton absorption, as observed in the transmission spectrum of the test beam. Therefore, in addition to the central hole due to the saturation of the direct transitions, the filling of the NC's state also quenches the indirect transitions to this state with the simultaneous emission of LO phonons (Fig. 14). Thus these phonon-assisted transitions give rise to the high-energy sideband.

The low-energy sideband is separated from the central hole by roughly the same energy (~ 18 meV) as the high-energy sideband. This sideband cannot be explained, however, by indirect transitions (absorption of a photon and a LO phonon) towards the preceding NC state directly filled by the pump beam since, at the low temperature of our studies, the number of LO phonons present in the crystals is very low. Another process very similar to the preceding one may, however, explain reasonably well the low-energy sideband. We have so far considered the direct excitation of NC's of a precise size by the pump beam, but we may also have at the same photon energy an indirect excitation (with the simultaneous emission of LO phonons) by the pump beam of NC's of a different size (Fig. 14). The state filling of this other NC ensemble may induce the saturation of the corresponding direct transitions, giving rise to the low-energy sideband. The slightly weaker energy separation of the low-energy sideband and the high-energy one of the central hole is contradictory with the fact that the LO-phonon energy is independent of the size of NC's (Fig. 3).

Another possibility could be the filling of the lowest excitonic state of nanocrystals of different sizes (larger) by the pumping of some higher excitonic states. These states could

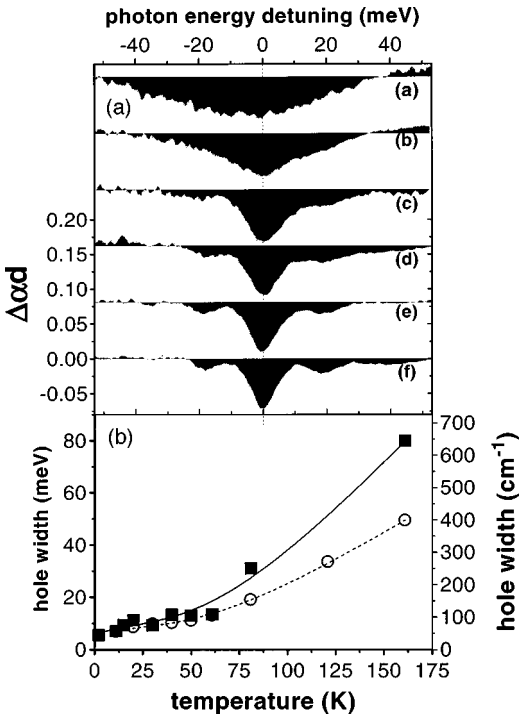

FIG. 15. Thermal evolution of SHB: The upper part (a) represents the persistent SH's at the following temperatures: (*a*) 160, (*b*) 80, (*c*) 60, (*d*) 40, (*e*) 20, and (*f*) 10 K for a sample containing NC's of 2.8 nm mean radius. The spectral position of the excitation is tuned as the absorption band shifts in order to maintain the excitation at the center of the SHs. In the lower part (b), the low-excitation limits of the widths of persistent (full squares) and transient (open circles) holes are plotted versus sample temperature. The continuous and dashed lines are fits obtained with Eq. (5).

arise from the splitting of the $Z_{1,2}$ degenerate excitonic state by electron-hole exchange interaction and by strain. We observed at low temperature a 8-meV splitting between the Γ_5 and the $\Gamma_3 \oplus \Gamma_4$ exciton states in the absorption spectra of large CuBr nanocrystals with a narrow size distribution. According to Refs. 15 and 16, this value has to be compared to the energy difference between the $\Gamma_3 \oplus \Gamma_4$ and Γ_5 exciton states of the bulk material when the long-range exchange interaction is neglected. For CuBr, one finds 5.8 meV.[19] Both values are comparable. The confinement could further increase the splitting between the excitonic states, however, only when the nanocrystal radius is smaller than the exciton Bohr radius.[20] This is not the case here. Additional strains would then be necessary to complete the process considered.

F. Temperature dependence of spectral-hole-burning structures

In order to clarify the effect of exciton-phonon interactions on SHB in small NC's, we studied SHB as a function of temperature. The persistent holes, for instance, have been measured from 10 to 160 K, as can be seen in Fig. 15. We tuned the dye laser to the center of the $Z_{1,2}$ absorption band (this band shifts to higher energies with increasing temperature) for each temperature because the spectral shape of the hole and its depth depend on which part of the absorption band is excited (see Sec. IV E). A small broadening of the central hole and a smoothing of the side holes are observed

up to about 60 K. At this critical temperature, the sidebands disappear abruptly and the width of the central hole starts to broaden rapidly with temperature (the persistent SHB's broaden more rapidly than transient ones). This dependence is similar to the temperature dependence of the emission linewidth (homogeneous width) observed in CuCl NC's.[21] We apply the function given in Ref. 21 to fit the experimental points of Fig. 15 [bearing in mind that the width of the spectral hole (FWHM) is twice the homogeneous width]:

$$\gamma_{\mathrm{hom}} = \gamma_0 + AT + Bn(T) + C[n(T)]^2, \tag{5}$$

where $n(T) = \{\exp(\hbar\Omega_{\mathrm{LO}}/k_B T) - 1\}^{-1}$ and the LO-phonon energy is $\hbar\Omega_{\mathrm{LO}} = 20.15$ meV. The first term is the temperature-independent width (the extrapolation of γ_{hom} to zero temperature). The second term represents the broadening by acoustic-phonon scattering in its high-temperature approximation. The last two terms are the contributions from one LO and two LO-phonon scatterings, which are important at higher temperatures. The best fit of our experimental data gives the following values of the parameters: $\gamma_0 = 3.3$ meV, $A = 0.040$ meV/K, $B = 49.3$ meV, and $C = 0.01$ meV for the transient holes and $\gamma_0 = 3.2$ meV, $A = 0.063$ meV/K, $B = 87.9$ meV, and $C = 0.008$ meV for the persistent ones. Compared to the size-selective measurements of Z_3 exciton emission in CuCl NC's,[21] the temperature dependence of the transient hole width gives a much higher value of γ_0. A is twice as high and B about 10% bigger. On the other hand, C is very low, almost negligible. As we do not extrapolate to very low excitation intensities, γ_0 is also larger than the value determined at the zero fluence limit (see Sec. IV D).

The difference of the hole widths between transient and persistent SH's increases with temperature (Fig. 13). We suppose it can be the effect of so-called spectral diffusion, a thermally stimulated relaxation in a glass matrix.[22]

V. CONCLUSIONS

Our pump- and-probe experiments confirm important differences in the behavior of ''big'' (mean radii $a \cong 12$, 9.5, and 5.1 nm) and ''small'' ($a \cong 3.9$ and 2.8 nm) CuBr NC's under a resonant excitation within the excitonic absorption band. The ''critical'' value of the NC radius at which we observe a change of behavior is about 3 or 4 times the Bohr radius of the bulk exciton. It coincides with the limit between the weak and intermediate regime of quantum confinement sometimes mentioned in the literature.

Big NC's show no SHB, only overall changes of the excitonic absorption band, which are explained well by the exciton-exciton interactions. The reason why SHB is not observed is probably due to the fact that the homogeneous and inhomogeneous excitonic linewidths are not very different.

In contrast, in small NC's we observe a relatively narrow spectral-hole burning. Both the persistent and transient SHB coexist. The spectral holes consist of the central hole at the excitation wavelength and pronounced sidebands. They are supposed to be due to a strong exciton-phonon interaction. In the ideal case, the central hole is a zero-phonon hole (ZPH) and its width should be twice the homogeneous width. The real width of the central hole, however, may be increased by low-frequency acoustic-phonon (of an energy of several meV) replicas that lie near the center of the hole and may be unresolved from the ZPH.[23]

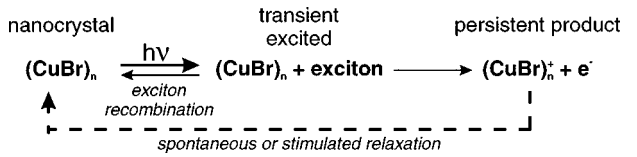

FIG. 16. Mechanisms of transient and persistent SHB in resonantly excited NC's.

The measured widths (FWHM) of SH's are always larger than twice the real homogeneous linewidth, due to various broadening mechanisms. So the experimental homogeneous width (for example, $\gamma_0 \cong 0.57$ meV at 3.091 eV at 2 K in 2.8-nm CuBr NC's) represents an upper limit of the real value and the derived [using Eq. (3)] dephasing time T_2 (2.300 ps) is a lower limit of the real T_2. Direct measurements of T_2 in the time domain by TFWM experiments (accumulated photon echo) using a frequency-doubled Ti:sapphire femtosecond laser give a value of 6.4 ps.

We observe a broadening of SH's when the NC's size decreases. The temperature broadening of the spectral holes is similar to the temperature dependence of the emission linewidth of CuCl NC's. Up to about 60 K the broadening is mainly driven by the acoustic-phonon scattering. The contribution from the LO-phonon scattering becomes important at higher temperatures.

Our experiments also indicate that the exciton-phonon interaction is relatively strong in CuBr NC's. The value $S \cong 1$ of the Huang-Rhys factor is deduced from the large Stokes shift between the excitonic absorption and the emission (corrected for reabsorption). The observation of strong LO and two LO-phonon lines in the resonantly excited Raman scattering spectra and of important side holes in the spectral profile of SH's is proof of a strong exciton-phonon coupling in CuBr NC's in the intermediate regime of the quantum confinement.

The picosecond dynamics of transient absorption changes gives a lifetime of the excitons in NC's. The values we found are 130 ± 20 ps and 1–100 ns for small and big CuBr NC's, respectively.

The mechanisms of transient and persistent SHB in resonantly excited NC's are presented in Fig. 16 and can be depicted in three stages: (i) *absorption* of a photon in the NC creates an exciton; (ii) *a transient excited state*, in which nanocrystal with an exciton inside has a shifted absorption spectrum during the lifetime of the free exciton, and (iii) *decay of an exciton*, in which the initial state of the NC can be restored by the exciton recombination. In small NC's, there is a large probability that this exciton gets trapped on the surface of the NC. This exciton can then be ionized, the electron or the hole being trapped separately on the interface of a NC and the glass matrix or inside the matrix. In such a way, the photochemical products of the excitation are created and stabilized. Consequently, the energetic spectrum of the NC matrix system is modified. A static electric field created by the separation of the electron and hole, for example, can cause an electro-optic Stark effect.

The photochemical mechanism of the persistent SHB in small CuBr NC's described is a straightforward hypothesis (similar to the one proposed by Masumoto[24]). More informa-

tion on the SHB mechanism deduced from a detailed investigation of persistent-hole-burning and hole-filling phenomena will be given elsewhere. The available data of hole-burning experiments are not yet sufficient, however, to have a clear understanding of their mechanism. Experiments with different matrices, SHB in the photoluminescence excitation and emission spectra, and SHB in external fields, as well as other experiments, are still needed.

ACKNOWLEDGMENTS

We appreciate valuable discussions with Dr. Riblet (IPCMS-GONLO, Strasbourg), Professor Hála, and Dr. Dian (Charles University, Prague). J.V. has received financial support from the French Ministry of Education (Contract No. 149151B and ''Réseau de Formation-Recherche, Europe Centrale et Orientale'').

---

*On leave from Charles University, Faculty of Mathematics and Physics, Department of Chemical Physics and Optics, Ke Karlovu 3, 121 16 Prague 2, Czech Republic. Electronic address: valenta@karlov.mff.cuni.cz

[1] N. Peyghambarian, B. Flugel, D. Hulin, A. Migus, M. Joffre, A. Antonetti, S. W. Koch, and M. Lindberg, IEEE J. Quantum Electron. **25**, 2516 (1989).

[2] P. Gilliot, J. C. Merle, R. Levy, M. Robino, and B. Hönerlage, Phys. Status Solidi B **153**, 403 (1989).

[3] M. G. Bawendi, W. L. Wilson, L. Rothberg, P. J. Carroll, T. M. Jedju, M. L. Steigerwald, and L. E. Brus, Phys. Rev. Lett. **65**, 1623 (1990).

[4] R. M. Macfarlane and R. M. Shelby, in *Persistent Spectral Hole-Burning: Science and Applications*, edited by W. E. Moerner (Springer-Verlag, Berlin, 1988).

[5] See, e.g., K. Naoe, L. G. Zimin, and Y. Masumoto, Phys. Rev. B **50**, 18 200 (1994); Y. Masumoto, L. G. Zimin, K. Naoe, S. Okamoto, T. Kawazoe, and T. Yamamoto, J. Lumin. **64**, 213 (1995).

[6] Zs. Bor, IEEE J. Quantum Electron. **16**, 517 (1980); S. Szatmani and F. P. Schafer, Appl. Phys. B: Photophys. Laser Chem. **33**, 95 (1984).

[7] A. I. Ekimov, Al. L. Efros, and A. A. Onduschenko, Solid State Commun. **56**, 921 (1985).

[8] A. I. Ekimov, Al. L. Efros, M. G. Ivanov, A. A. Onduschenko, and S. K. Shumilov, Solid State Commun. **69**, 565 (1989).

[9] U. Woggon, O. Wind, W. Langbein, O. Gogolin, and C. Klingshirn, J. Lumin. **59**, 135 (1994).

[10] J. Friedrich and D. Haarer, Angew. Chem. **23**, 113 (1984).

[11] S. Lewonczuk, J. Ringeissen, and S. Nikitine, J. Phys. (Paris) **32**, 941 (1971).

[12] C. Marangé, A. Bivas, R. Lévy, J. B. Grun, and C. Schwab, Opt. Commun. **6**, 138 (1972).

[13] U. Woggon, F. Henneberger, and M. Müller, Phys. Status Solidi B **150**, 641 (1988).

[14] R. Lévy, P. Gilliot, L. Mager, and B. Hönerlage, Phys. Rev. B **44**, 11 286 (1991).

[15] L. Belleguie and L. Bányai, Phys. Rev. B **44**, 8785 (1991).

[16] B. Hönerlage, U. Rössler, Vu Duy Phach, A. Bivas, and J. B. Grün, Phys. Rev. B **22**, 297 (1980).

[17] J. Valenta, J. Moniatte, P. Gilliot, R. Lévy, B. Hönerlage, and A. I. Ekimov, Appl. Phys. Lett. **70**, 680 (1997).

[18] J. Osadko, Phys. Rep. **206**, 43 (1991).

[19] T. Takagahara, Phys. Rev. B **47**, 4569 (1993).

[20] R. Romestain and G. Fishman, Phys. Rev. B **49**, 1774 (1994).

[21] T. Itoh and M. Furumiya, J. Lumin. **48&49**, 704 (1991).

[22] R. Jankowiak, J. M. Hayes, and G. J. Small, Chem. Rev. **93**, 1471 (1993).

[23] S. Okamoto and Y. Masumoto, J. Lumin. **64**, 253 (1995).

[24] Y. Masumoto, J. Lumin. **70**, 386 (1996).